# Lagrangian Refined Kolmogorov Similarity Hypothesis for Gradient Time Evolution and Correlation in Turbulent Flows

Huidan Yu* and Charles Meneveau†

*Department of Mechanical Engineering, Institute for Data Intensive Engineering and Science, Johns Hopkins University, Baltimore, Maryland 21218, USA*

(Received 14 November 2009; published 25 February 2010)

We study time evolution of velocity and pressure gradients in isotropic turbulence by quantifying their autocorrelation functions and decorrelation time scales. The Lagrangian analysis uses data in a public database generated by direct numerical simulation at a Reynolds number $\mathrm{Re}_\lambda \approx 433$. It is confirmed that when averaging over the entire domain, correlation functions decay on time scales on the order of the global Kolmogorov turnover time scale. However, when performing the analysis in different subregions of the flow, turbulence intermittency leads to large spatial variability in the decay time scales. Remarkably, excellent collapse of the autocorrelation functions is recovered when using a locally defined Kolmogorov time scale. This provides new evidence for the validity of Kolmogorov's refined similarity hypothesis, but from a Lagrangian viewpoint that provides a natural frame to describe the dynamics of turbulence.

DOI: 10.1103/PhysRevLett.104.084502 PACS numbers: 47.27.E−

Understanding the universal features of the dynamics of turbulence [1,2] continues to be a formidable problem in classical and statistical physics. The original Kolmogorov 1941 theory relied on the overall averaged dissipation rate $\langle\epsilon\rangle$ to predict, among others, the scaling properties of the energy spectrum. It was extended to account for intermittency by the introduction of the refined Kolmogorov similarity hypothesis (RKSH) [3]. In this extension, attention is placed on conditional statistics based on the locally averaged dissipation rate in some particular subregion of the flow, such as a sphere or box of size $r$. This local dissipation rate, usually denoted by $\epsilon_r$, is defined according to $\epsilon_r(\mathbf{x}) = V^{-1}\int_{\mathcal{R}_r(\mathbf{x})} 2\nu[S_{ij}(\mathbf{x}')]^2 d^3\mathbf{x}'$, where $V$ is the volume of the subregion $\mathcal{R}_r(\mathbf{x})$ of size $r$ centered at $\mathbf{x}$, $\nu$ is the kinematic viscosity of the fluid, and $S_{ij}$ is the strain-rate tensor defined as $S_{ij} = (\partial u_i/\partial x_j + \partial u_j/\partial x_i)/2$ (where $u_i$ is the velocity field). The longitudinal velocity increment at scale $r$ is defined as $\delta_r u = [u_i(\mathbf{x}+\mathbf{r}) - u_i(\mathbf{x})](r_i/r)$, and the RKSH states that in the inertial range of turbulence the statistics of $\delta_r u$ depend on $r$ and $\epsilon_r$ so that from dimensional analysis moments of $\delta_r u$, conditioned upon a fixed value of $\epsilon_r$ will scale as $\langle\delta_r u^p|\epsilon_r\rangle = C_p(r\epsilon_r)^{p/3}$ according to Kolmogorov's 1941 postulate. Anomalous scaling then results from the additional global averaging and anomalous scaling behavior of moments of $\epsilon_r$.

Extensive literature to test RKSH has focused mainly on velocity increments [4–8] or acceleration [9]. In recent years there has been growing attention placed in the dynamical evolution of the velocity-gradient tensor $\mathbf{A}$ ($A_{ij} \equiv \partial u_i/\partial x_j$) due to the fact that $\mathbf{A}$ provides rich information about the topological and statistical properties of small-scale structure in turbulence. The Lagrangian time evolution of $\mathbf{A}$ can be obtained by taking the gradient of the Navier-Stokes equation [10]:

$$\frac{dA_{ij}}{dt} = -A_{ik}A_{kj} - \frac{\partial^2 p}{\partial x_i \partial x_j} + \nu\frac{\partial^2 A_{ij}}{\partial x_k \partial x_k}, \qquad (1)$$

where $d/dt$ stands for Lagrangian material derivative and $p$ is the pressure divided by the density of the fluid. The first term on the right-hand side of Eq. (1) denotes the nonlinear self-interaction of $\mathbf{A}$, the second term is the pressure Hessian, and the third is the viscous term. Assuming the pressure Hessian is isotropic (i.e., neglecting $\partial^2_{ij}p - \partial^2_{kk}p\,\delta_{ij}/3$) and neglecting the viscous term lead to a closed formulation for $\mathbf{A}$, the so-called restricted-Euler (RE) equation, which has analytical solutions for the full tensor-level time history. Remarkably this simple system is already sufficient to explain a number of nontrivial geometrical trends found in real turbulence [10,11]. Nevertheless, the RE system leads to nonphysical finite-time singularities because the self-stretching is not constrained by any energy exchange or loss mechanism in the system. To develop models for such energy exchanges, there is a need to better understand the time evolution of $\mathbf{A}$, as one follows fluid particles across a turbulent flow. As will be shown in this Letter, the RKSH can play a crucial role in determining the characteristic time scales of this evolution in different parts of the flow.

Much effort at regularizing the RE system to avoid nonphysical singularities has been made [12–17] in the past two decades. Despite progress, the inability to fully account for the anisotropic pressure Hessian and viscous effects continues to limit the accuracy of the existing models for the evolution of velocity-gradient tensor [18]. In various models of the Lagrangian dynamics [12,15,16,18], the characteristic correlation times along Lagrangian trajectories and their scaling with Reynolds number play a central role. For instance in the model based on the "recent fluid deformation closure" [16] the

 

Lagrangian pressure Hessian tensor is assumed isotropic, based on the idea that any causal relationship between initial and present orientations will be lost after a characteristic Lagrangian correlation time scale of the tensor $\mathbf{A}$. The usual expectation is that the characteristic correlation time scale of $\mathbf{A}$ is the Kolmogorov time scale $\tau_K = (\nu/\langle\epsilon\rangle)^{1/2}$.

Since the dynamical equation for the velocity-gradient tensor $\mathbf{A}$ [Eq. (1)] and the existing models [12–17] are written for the full tensor, it is of interest to quantify the temporal correlation function of each tensor element but to do so in a fashion that is coordinate system invariant. We thus use the tensor-based Lagrangian time-correlation function of a second-rank tensor $\mathbf{C}$, defined as

$$\rho_{\mathbf{C}}(\tau) \equiv \frac{\langle C_{ij}(t_0)C_{ij}(t_0+\tau)\rangle}{\sqrt{\langle (C_{mn}(t_0))^2\rangle\langle (C_{pq}(t_0+\tau))^2\rangle}}, \qquad (2)$$

where $\tau$ is the time-lag along Lagrangian trajectories and $\langle\ldots\rangle$ represents volume averaging for homogeneous turbulence and where summation over repeated indices is understood. Here tensor elements are assumed to have zero mean for isotropic turbulence. For a statistically steady-state process, when $\rho_{\mathbf{C}}(\tau)$ does not depend upon $t_0$, averaging can also be done over $t_0$. The correlation function $\rho_{\mathbf{C}}(\tau)$ provides a frame-invariant description of the autocorrelation structure of tensor elements, appropriately summed over all directions.

The fluid acceleration is another variable of great interest. The Lagrangian velocity and acceleration statistics have been investigated both experimentally [19] and numerically [20,21]. The acceleration is associated more closely with inertial-range and small-scale structures. It has been established that the acceleration is dominated by the pressure gradient $\nabla p$ and viscous forces are negligible away from boundaries [22,23]. Therefore, we study the time correlations of pressure gradient. Specifically, similar to the tensor correlation function defined in Eq. (2), for the pressure gradient correlation $\rho_{\nabla p}(\tau)$ we use the inner product of the vector at $t_0$ and $t_0+\tau$.

We measure $\rho_{\mathbf{C}}(\tau)$ for $\mathbf{C} = \mathbf{A}$, $\mathbf{S}$, or $\mathbf{\Omega}$ [$\Omega_{ij} = (A_{ij} - A_{ij})/2$] and $\rho_{\nabla p}(\tau)$ using data from pseudospectral direct numerical simulation of forced isotropic turbulence on a $1024^3$-node periodic domain, with $\mathrm{Re}_\lambda \approx 433$. The 27 terabytes of data are stored in a public database format [24] and can be accessed using web-service tools. We track fluid particles and extract Lagrangian information, such as velocity and pressure gradients, along the fluid particle trajectories through the second-order Runge-Kutta particle-tracking algorithm [25]. The interpolation of required velocities uses 8th-order Lagrange polynomials in space and piecewise cubic Hermite polynomial interpolation in time, as implemented in the predefined functions in the database [26]. Data volumes are stored in the database every $\Delta t_{db} = 0.002$ (in units of the simulation, in which $u' = 0.681$, the box size is $L = 2\pi$, $\nu = 0.000\,185$ and $\tau_K = 0.0446$). Our particle tracking uses $\Delta t = 0.009\tau_K$, allowing highly accurate tracking with a root-mean-square CFL number of $\Delta t u'/\Delta x = 0.044$.

The Lagrangian time correlations for $\mathbf{S}$ and $\mathbf{\Omega}$ are shown as open squares in Fig. 1(a) (the meaning of the other lines are explained below). As can be seen, the strain-rate autocorrelation decays fairly rapidly and reaches almost zero near 5–6 Kolmogorov time scales, much faster than that of the rotation rate, see also [12].

It is known [2] that turbulence is highly intermittent, with regions displaying strong fluctuations, interspersed with less turbulent regions. In order to study intermittency from the viewpoint of the Lagrangian time evolution, we compute the correlation functions based on fluid particles that originate from various subregions of the flow. The subregions are characterized by the local dissipation rate $\epsilon_r$. We thus define the conditional time-correlation functions based on $\epsilon_r$. In Eq. (2), the three global averages are replaced by conditional averages, e.g., $\langle C_{ij}(t_0)C_{ij}(t_0+\tau)\rangle \rightarrow \langle C_{ij}(t_0)C_{ij}(t_0+\tau)|\epsilon_r\rangle$. In these averages the initial position of particles contributing to the average at time $t_0$ are sampled from several local boxes of size $r$ that have a prescribed locally averaged dissipation rate $\epsilon_r$ (in practice a range of values in a prescribed "bin" is used). We consider four scales $r$ in the inertial range of turbulence corresponding to 16, 32, 64, and 128 grid points of the DNS or $r = 34\eta_K$, $68\eta_K$, $136\eta_K$, and $272\eta_K$, respectively, where $\eta_K$ is the Kolmogorov length scale. Four bins of $\epsilon_r/\langle\epsilon\rangle$ values are chosen, centered at $\epsilon_r/\langle\epsilon\rangle =$ 0.08, 0.2, 1.0, and 1.6 for 16 cubes, 0.1, 0.2, 1.0, and 1.6 for 32 cubes, and 0.4, 0.6, 1.0, and 1.2 for 128 cubes. For scale $r = 136\eta_K$ (64 cube), we have an extra set of five bins which are centered at $\epsilon_r/\langle\epsilon\rangle = 0.4$, 0.5, 0.7, 0.9, and 1.5. The overall mean dissipation rate over the entire data set is $\langle\epsilon\rangle = 0.093$ [26].

To illustrate the situation, in Fig. 2(a) we show 12 representative 64 cubes placed inside the $1024^3$ domain,

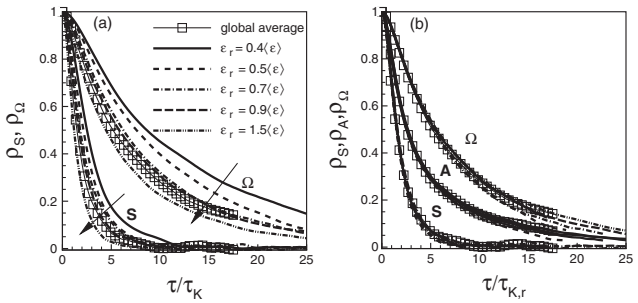


FIG. 1. Lagrangian autocorrelations of strain- and rotation-rate tensors computed from Eq. (2). Open squares are for global average over randomly located particles, whereas different lines correspond to subregions of the flow characterized by certain $\epsilon_r$. Time lag is normalized using (a) the global Kolmogorov time scale $\tau_K$ and (b) the local time scale $\tau_{K,r}$.

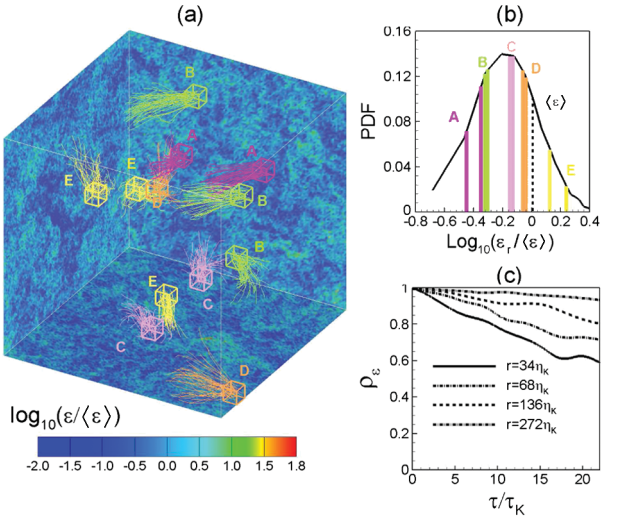


FIG. 2 (color). (a) Sample particle trajectories starting from 12 randomly selected 64 cubes (5 bins) characterized by local dissipation rate $\epsilon_r$ at the initial time. Contours on the background planes show local dissipation rate (at the initial time) in logarithmic units, showing its intermittent but structured distribution at the smallest scales of the flow. (b) PDF of the dissipation rate together with the bins or $\epsilon_r$ values used for the conditional averaging. (c) Lagrangian time-correlation function between dissipation rate averaged over all fluid particles that start in a cube, for four different values of $r$.

with 50 sample fluid particle trajectories emanating from each and progressing during a time equal to $27\tau_K$. The required averages are taken over all these trajectories as well as over several cubes for which $\epsilon_r$ is in a bin's prescribed range. The probability density function (PDF) of the dissipation rate is shown in Fig. 2(b) together with the bins of $\epsilon_r$ values used for the conditional averaging.

For the case of $r = 136\eta_K$ (64 cube), the various lines in Fig. 1(a) show the conditional autocorrelation functions so computed, plotted as function of time delay scaled by global Kolmogorov time scale $\tau_K$. Averages are evaluated over $6 \times 10^3$ particles in each bin. Tests varying the number of particles show that the autocorrelation functions are well converged with this number of particles. There are noticeable differences in the results depending on $\epsilon_r$, for both the $\mathbf{S}$ and $\mathbf{\Omega}$ autocorrelation functions. For larger values of $\epsilon_r$, i.e., in regions of more intense turbulence activity, the decay rate of the autocorrelation functions is faster. This shows that the global Kolmogorov time scale $\tau_K = (\nu/\langle\epsilon\rangle)^{1/2}$ does not determine the local evolution of patches of turbulence, even in a statistical sense when conditional averaging is used that segregates different types of fluid regions.

As a next step, consistent with the RKSH, we define a "local Kolmogorov time scale" based on the local dissipation rate according to

$$\tau_{K,r} = (\nu/\epsilon_r)^{1/2}. \tag{3}$$

A Lagrangian version of the RKSH would state that the temporal autocorrelation functions should be a universal function of a time-delay $\tau$ normalized by a local Kolmogorov time scale $\tau_{K,r}$. Results shown in Fig. 1(b) thus scaled by the local time scale for each tensor show excellent collapse. In this plot we also show the autocorrelation for the velocity-gradient tensor $\mathbf{A}$ which falls between the results of its symmetric and antisymmetric parts. Again, the autocorrelation of the rotation-rate tensor decays much more slowly than that of the strain-rate tensor. Figure 3 shows results for the pressure gradient. Also here, the collapse is much more improved when using the local time scale that corresponds to the local dissipation rate, showing that the Lagrangian RKSH works for both the velocity and pressure gradients, the latter corresponding closely to the fluid acceleration [22,23]. In order to quantify the relevance of the initial value of $\epsilon_r$ in each cube, we evaluate the time-correlation function between $\epsilon_r$ and the subsequent dissipation rate averaged over all the fluid particles from each cube. The decay is quite slow, as is seen in Fig. 2(c).

We point out that in a recent work [27] the Lagrangian RKSH has also been shown to hold in the context of moments of two-time velocity increments. In their analysis, the authors use a rate of dissipation $\epsilon_r$ averaged over *temporal* domains of duration $\tau$ along the particle trajectory. The "fully Lagrangian" quantity $\epsilon_\tau$ averages, and thus connects, dissipation at various times. From a different, perhaps complementary point of view, the present analysis based on the more traditional spatial average of dissipation at a single (initial-condition) time facilitates interpreting the results in terms of "causality" based on a fixed initial condition.

Next, we explore the validity of the Lagrangian KRSH for different box sizes $r$. Figure 4 shows the autocorrelations of strain-rate tensor $\rho_{\mathbf{S}}$ for the four box sizes $r$ and $\epsilon_r$ described above. Now the scatter is even more pronounced in (a) where time lag is normalized by the global averaged Kolmogorov time scale $\tau_K$, mainly due to the fact that the range of values of $\epsilon_r$ for smaller values of $r$ is larger due to intermittency. Once again, excellent collapse can be ob-

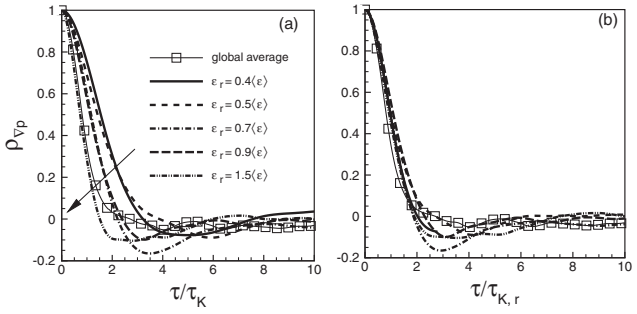


FIG. 3. Lagrangian autocorrelations of pressure gradient. The time lag is normalized using (a) global time scale $\tau_K$ (the arrow is for increasing $\epsilon_r$), and (b) local time scale $\tau_{K,r}$.

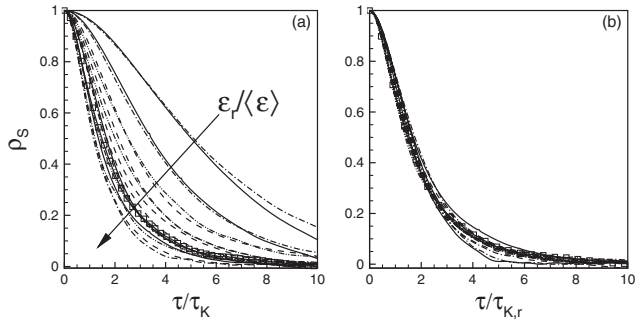


FIG. 4. Lagrangian autocorrelations of **S** computed from Eq. (2) for four box sizes $r$ in the inertial range, and for different $\epsilon_r$. Solid lines: 16 cube; dash-dotted lines: 32 cube; dash-dashed lines: 64 cube; dash-dot-dotted lines: 128 cube; open squares: global average. In (a) time is scaled using $\tau_K$, in (b) using the local time scale $\tau_{K,r}$.

served in (b) where the time lag is normalized by the local Kolmogorov time-scales $\tau_{K,r}$, even though the curves correspond to different $r$ and $\epsilon_r$ values. This is confirmed further by comparing the results with similar local $\epsilon_r$ values but different $r$: e.g., the first two curves from the right to left shown in Fig. 4(a) correspond to $\epsilon_r/\langle\epsilon\rangle = 0.08$ for a 16 cube and 0.1 for a 32 cube and they collapse quite well. The strain-rate correlation time scale obtained from integrating the area under the curve in Fig. 4(b) is $\mathcal{T}_{S,r} = 2.07\tau_{K,r}$. Good collapse (not shown) is obtained for rotation-rate tensor also.

Present results provide a new and more dynamical interpretation of the Kolmogorov similarity hypothesis: when focusing on particular subregions of turbulence, the dynamics proceed according to time scales dictated by the locally averaged rate of dissipation. The classical view of the RKSH focused on the moments of velocity increments in turbulent fields that had already developed due to past dynamics. Here we have shown that the dynamical time evolution of turbulence, its rate of change, and associated decorrelation time scale, depends on the local rate of dissipation, averaged over a volume comparable to the volume containing the sample of initial particle locations. Results also suggest that Lagrangian models (e.g., for the velocity-gradient tensor [16] or the acceleration [28]) that require specification of a characteristic time scale should not use the global, but the local time scale.

We thank the Keck Foundation for postdoctoral support (H. Yu.), the National Science Foundation (ITR-0428325 and CDI-0941530) for its support of the public database, and Professor G. L. Eyink for insightful comments.

*hyu36@jhu.edu
†meneveau@jhu.edu

[1] A. N. Kolmogorov, Dokl. Akad. Nauk SSSR **30**, 301 (1941); Proc. R. Soc. A **434**, 9 (1991).
[2] U. Frisch, *Turbulence: The Legacy of A. N. Kolmogorov* (Cambridge University Press, Cambridge, U.K., 1995).
[3] A. N. Kolmogorov, J. Fluid Mech. **13**, 82 (1962).
[4] G. Stolovitzky, P. Kailasnath, and K. R. Sreenivasan, Phys. Rev. Lett., **69**, 1178 (1992).
[5] S. Chen, G. D. Doolen, R. H. Kraichnan, and Z.-S. She, Phys. Fluids A **5**, 458 (1993).
[6] G. Stolovitzky and K. R. Sreenivasan, Rev. Mod. Phys. **66**, 229 (1994).
[7] S. Chen, G. D. Doolen, R. H. Kraichnan, and L.-P. Wang, Phys. Rev. Lett. **74**, 1775 (1995).
[8] E. S. C. Ching, H. Guo, and T. S. Lo, Phys. Rev. E **78**, 026303 (2008).
[9] P. K. Yeung, S. B. Pope, A. G. Lamorgese, and D. A. Donzis, Phys. Fluids **18**, 065103 (2006).
[10] P. Vieillefosse, J. Phys. (Paris) **43**, 837 (1982).
[11] B. J. Cantwell, Phys. Fluids A **4**, 782 (1992).
[12] S. S. Girimaji and S. B. Pope, Phys. Fluids A **2**, 242 (1990).
[13] J. Martin, C. Dopazo, and L. Valĩno, Phys. Fluids **10**, 2012 (1998).
[14] M. Chertkov, A. Pumir, and B. I. Shraiman, Phys. Fluids **11**, 2394 (1999).
[15] E. Jeong and S. S. Girimaji, Theor. Comput. Fluid Dyn. **16**, 421 (2003).
[16] L. Chevillard and C. Meneveau, Phys. Rev. Lett. **97**, 174501 (2006).
[17] L. Biferale, L. Chevillard, C. Meneveau, and F. Toschi, Phys. Rev. Lett. **98**, 214501 (2007).
[18] M. M. Afonso and C. Meneveau, Physica D (Amsterdam) doi:10.1016/j.physd.2009.03.001 (2009).
[19] A. La Porta, G. A. Voth, A. M. Crawford, J. Alexander, and E. Bodenschatz, Nature (London) **409**, 1017 (2001).
[20] P. K. Yeung, Annu. Rev. Fluid Mech. **34**, 115 (2002).
[21] F. Toschi and E. Bodenschatz, Annu. Rev. Fluid Mech. **41**, 375 (2009).
[22] P. Vedula and P. K. Yeung, Phys. Fluids **11**, 1208 (1999).
[23] X. Liu and J. Katz, Exp. Fluids **41**, 227 (2006).
[24] http://turbulence.pha.jhu.edu.
[25] P. K. Yeung and S. B. Pope, J. Comput. Phys. **79**, 373 (1988).
[26] Y. Li, E. Perlman, M. Wan, Y. Yang, R. Burns, C. Meneveau, R. Burns, S. Chen, A. Szalay, and G. Eyink, J. Turbul. **9**, 31 (2008).
[27] R. Benzi, L. Biferale, E. Calzavarini, D. Lohse, and F. Toschi, Phys. Rev. E **80**, 066318 (2009).
[28] A. G. Lamorgese, S. B. Pope, P. K. Yeung, and B. L. Sawford, J. Fluid Mech. **582**, 423 (2007).